Synthesis and Characterization of $Cu_{11}V_6O_{26}$ as High–Capacity Cathodes for Lithium Secondary Batteries via a Wet–Chemistry Route

[1]CHAO YUAN, [1]BINQIANG MA, [1]XIN LI, [2]SUHONG LÜ AND [3]XIAOYU CAO*
[1]*College of Sciences, Henan Agricultural University, Zhengzhou 450002, P.R. China*
[2]*College of Information and Management Sciences, Henan Agricultural University, Zhengzhou 450002, P.R. China*
[3]*School of Chemistry and Chemical Engineering, Henan University of Technology, Zhengzhou 450001, P.R. China*

(Received on 8th November 2008, accepted in revised form 12th October 2009)

Summary: The cathode material of $Cu_{11}V_6O_{26}$ has been synthesized for the lithium secondary batteries *via* the wet-chemistry method. The as-prepared powders were characterized by powder X-ray diffraction (XRD), scanning electron microscope (SEM) and laser particle size analysis (LPSA). The electrochemical performances were evaluated by the galvanostatic discharge-charge and cyclic voltammetry technique. These results revealed that $Cu_{11}V_6O_{26}$ powder could be formed at a temperature as low as 300 °C, and its particle size was smaller and distributed in a narrower range compared to the other powders synthesized at 400 °C and 500 °C. The initial discharge capacity of the powder synthesized at 300 °C whose $D_{50\%}$ was only 24.251μm was 318.2 mAh/g. It was also found that a severe structure modification of $Cu_{11}V_6O_{26}$ powder might take place after the first cycle according to cyclic voltammetry test, which should be responsible for its irreversible capacity.

Introduction

The great demand for lithium ion batteries as power source for the electronics devices, such as cellular phones and various portable electrical products has triggered extensive research on cathode materials with high specific energy. Increasing the specific energy of lithium ion batteries is not only an ongoing pursuit for many scientists but also of great interests to the electric vehicle industry. To reach the goal of a high specific energy, two essential requirements must be met by cathode materials, *i.e.*, high discharge specific capacity and average working voltage [1].

Previously, copper vanadium oxides (CVOs) have shown promise for use as cathodes in lithium secondary batteries due to their high specific capacities and energy densities [2-14]. Among CVOs, $Cu_{11}V_6O_{26}$ is one of potential cathode candidate for the lithium secondary batteries because of its high discharge capacity [4]. However, the solid-state synthesis of $Cu_{11}V_6O_{26}$ starting from CuO and V_2O_5 powders is a relative difficult and complicated process, since it requires an elevated heating temperature, long reaction time and repeated calcination procedure [4]. At such extreme reaction condition, it is difficult to control an accurate ratio of copper to vanadium atom owing to the reactants evaporation and the corrosion of molten V_2O_5 to the crucible. At the same time, the elevated calcination temperature and long reaction time will lead to large particle size and uncontrolled morphology, which can deteriorate the electrochemical performances of cathode materials.

Considering the above–mentioned shortcomings of the solid-state synthesis method, in this work, the wet chemistry synthesis method has been applied in the preparation of $Cu_{11}V_6O_{26}$. To the best of our knowledge, there has not been previously reported on the synthesis of $Cu_{11}V_6O_{26}$ by this soft synthesis method. The structure, morphology and electrochemical properties of the as-prepared $Cu_{11}V_6O_{26}$ powders have been studied.

Results and Discussion

$Cu_{11}V_6O_{26}$ precursor is sintered at series temperature for 10 h, and the XRD profiles of these powders are shown in Fig. 1. The powder made at 300 °C shows similar diffraction pattern to the powders obtained at higher temperatures, and these powders are identified to be the triclinic system with

*To whom all correspondence should be addressed.

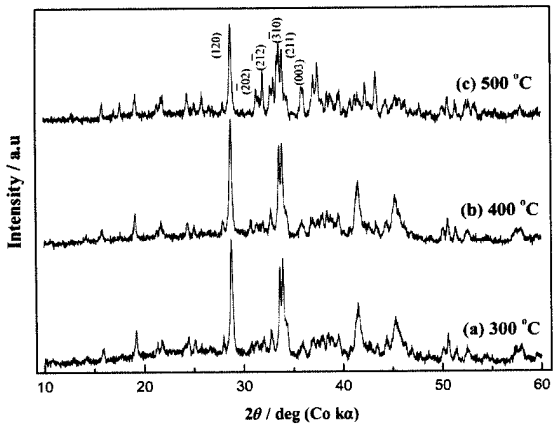

Fig. 1: XRD patterns of $Cu_{11}V_6O_{26}$ powders obtained at different temperatures.

space group $P1$. The XRD results in Fig. 1 also confirm the hypothesis that the temperature required for the formation of $Cu_{11}V_6O_{26}$ is lowered when the wet chemistry synthesis method is adopted (a temperature of above 700 °C is essential if $Cu_{11}V_6O_{26}$ is prepared via the solid-state reaction). The cause for the formation of $Cu_{11}V_6O_{26}$ powder at a much lower temperature should be multifactorial. First, during the synthesis of $Cu_{11}V_6O_{26}$ precursor, the contact of reactants in fluid slurry is close and uniform, and the heat exchange can be carried out easily and quickly. So, the crystal nucleuses of $Cu_{11}V_6O_{26}$ are likely to be partly formed in the precursor. In the subsequent heating process, only a small quantity of heat can be guaranteed for the growth of the crystal nucleuses and the formation of $Cu_{11}V_6O_{26}$ phase. In addition, metal–oxalate complexes can be first formed when the oxalic acid is added to the wet chemical system. When the reaction system is heated, the metal–oxalate complexes are burned intensely and a great deal of heat are released because of their flammability, which also leads to the lower synthetic temperature.

SEM images of the $Cu_{11}V_6O_{26}$ powders synthesized at series temperature for 10 h are shown in Fig. 2. In the case of $Cu_{11}V_6O_{26}$ powder (Fig. 2a) obtained at 300 °C, small nano-/micro-sized crystallites with the somewhat aggregation can be observed. This is because that the powder obtained at low temperature is bonded with certain crystal water.

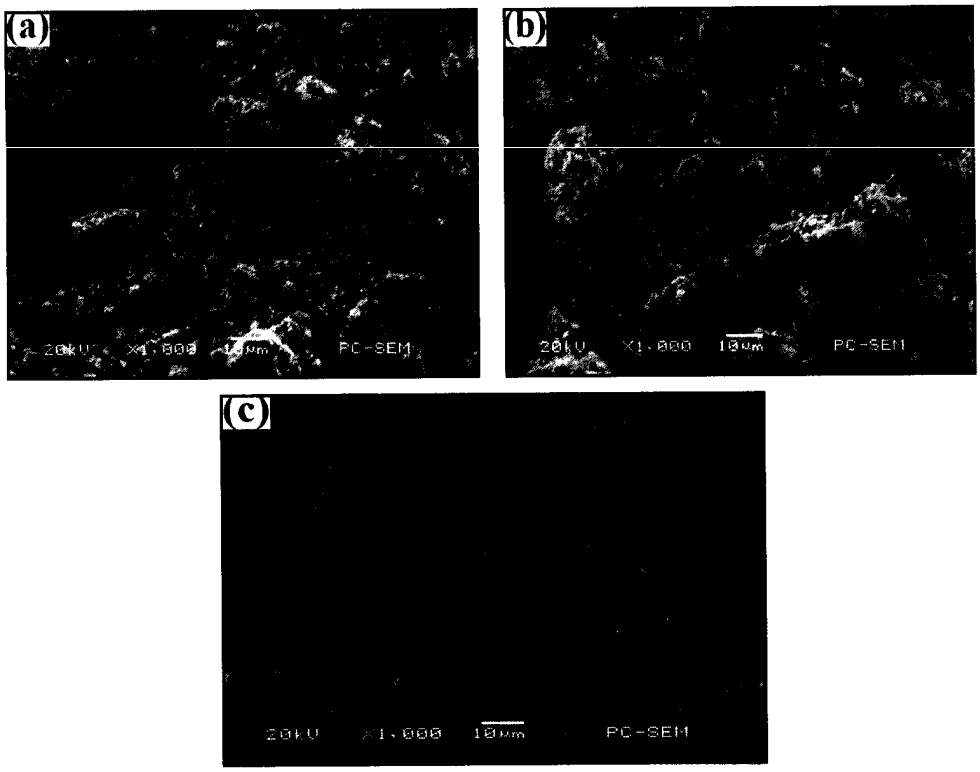

Fig. 2: SEM images of $Cu_{11}V_6O_{26}$ powders obtained at different temperatures (a) 300 °C, (b) 400 °C, (c) 500 °C.

When the sintering temperature increases to 500 °C, the particle sizes become much larger and the irregular platelet shaped particles are formed due to the further dehydration. Also, the material prepared at 300 °C and 400 °C presents somewhat porous particles, which may be caused by the existence of oxalic acid. CO_2 and H_2O gas generated by metal–oxalate complexes can escapes from the matrix complexes when the $Cu_{11}V_6O_{26}$ precursor is heated, which gives rise to the porous electrode material. Because the intercalation process of Li^+ ion into the cathode materials is a diffusion process, so this morphological characteristic may facilitate electrolyte soaking into particles and thus improve the diffusion kinetics of Li^+ into/out of $Cu_{11}V_6O_{26}$ due to the porosity.

It should be clarified that particle size analysis can exhibit the entire picture of the pattern where the particles are distributed in the bulk but SEM analysis only gives the magnification of the selected portion of the powder and represents the averaged out size of the particles. In order to elucidate the particle size distribution of the as-synthesized powders, the LPSA is conducted and the result is shown in Fig. 3. It displays the variation of volume fraction of the particle with the particle size. As seen in Fig. 3, the particle size of the powder obtained at 300 °C is distributed in a much narrower range compared to the powder obtained at 400 °C and 500 °C. Table-1 summarizes the selected particle size distribution dada of $Cu_{11}V_6O_{26}$ powders. $D_{10\%}$ denotes the maximal particle size when the volume ratio of the cumulate volume to the total volume amounts to 10%. The meaning of $D_{50\%}$ and $D_{90\%}$ can be analogical. It is noticed that the powder synthesized at 300 °C is superior to the other powders in the small and uniform-distributed particle size, and its average particle size is only 24.251 μm.

The first discharge curves of the $Cu_{11}V_6O_{26}$ powders heat-treated at different temperatures are shown in Fig. 4. According to Fig. 4, the powders heated at 300 °C, 400 °C and 500 °C have the first

Table-1: Particle size distribution of $Cu_{11}V_6O_{26}$ powders obtained at different heating temperatures.

Powders	$D_{10\%}$ (μm)	$D_{50\%}$ (μm)	$D_{90\%}$(μm)
300 °C	1.936	24.251	71.627
400 °C	3.920	31.870	86.905
500 °C	7.521	38.299	94.716

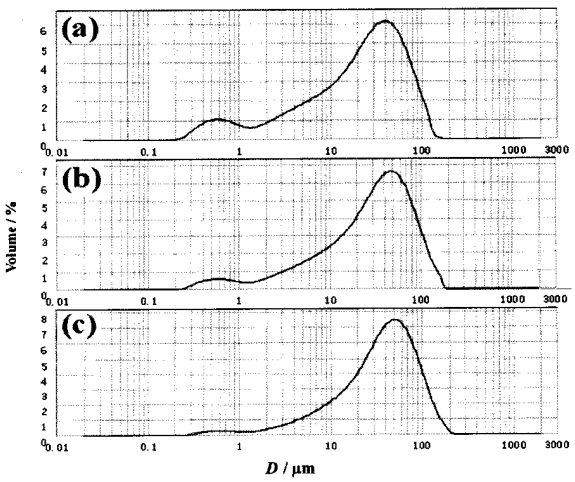

Fig. 3: Particle size distribution curves of $Cu_{11}V_6O_{26}$ powders obtained at different temperatures (a) 300 °C, (b) 400 °C, (c) 500 °C.

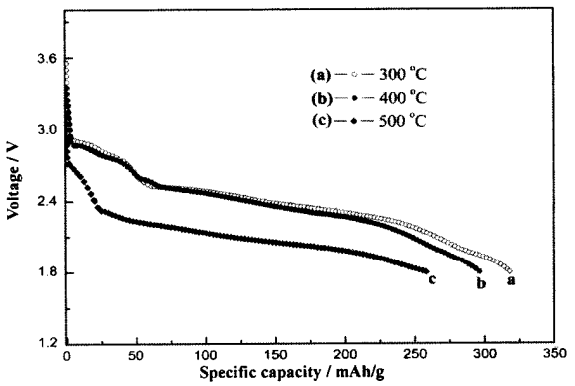

Fig. 4: The first discharge curves of $Cu_{11}V_6O_{26}$ powders treated at different temperatures (a) 300 °C, (b) 400 °C, (c) 500 °C.

discharge capacity of 318.2 mAh/g, 296.6 mAh/g and 258.5 mAh/g, respectively. These discharge capacities are much higher than that of the commercialized $LiCoO_2$ powders. Meanwhile, there are several discharge plateaus in the voltage curves for the lithium intercalation of $Cu_{11}V_6O_{26}$ powders synthesized at 300 °C and 400 °C. Among these discharge plateaus, two main voltage plateaus at about 2.8 V and 2.38 V can be clearly observed. With the increase in heat-treatment temperature, only two voltage plateaus can be observed for the powder heat-treated at 500 °C and shift in much lower potential direction. The difference in the

electrochemical performance between these powders is closely relates to the particle size. As was reported, the smaller grain size will result in a shorter diffusion path of Li^+ ions and effectively restrains the electrode polarization [11]. On the contrary, the higher heat-treatment temperature will lead to the formation of larger-sized grains and it makes Li^+ ions diffusion become the control step for the overall electrochemical reaction. Thus, we can explain the fact that the powder heat-treated at 500 °C displays a lower discharge capacity than the powders obtained at 300 °C and 400 °C.

Fig. 5 shows the first four cycles of the powder prepared at 300 °C. As illustrated in Fig. 5, the material suffers a large decrease in the discharge capacity during the first two cycles and an initial irreversible capacity loss is 89 mAh/g. From the second cycle, discharge capacity stabilizes at about 200 mAh/g. According to M. Eguchi [4], metallic copper is preferentially formed during the early states of discharge. The formation of metallic copper at least brings about the two different effects. First, it contributes to a part of discharge capacity and increases the electronic conductivity of $Cu_{11}V_6O_{26}$ matrix during discharge, which leads to a large amount of Li^+ ions intercalation. On the other hand, the structural modifications of $Cu_{11}V_6O_{26}$ material caused by the reduction of Cu (II) probably leads to a capacity fading.

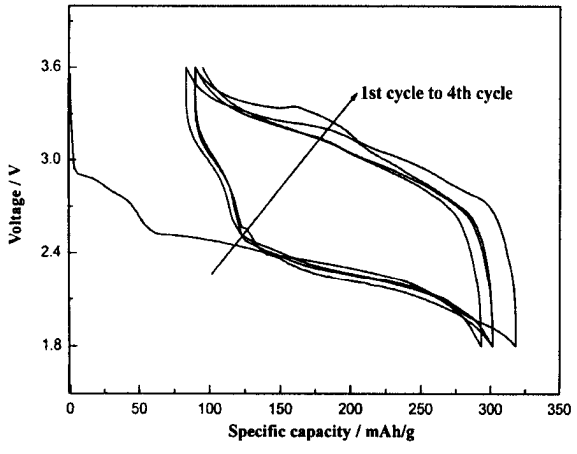

Fig. 5: The discharge–charge curves of $Cu_{11}V_6O_{26}$ powder obtained at 300 °C.

Fig. 6 shows the CV curves of $Cu_{11}V_6O_{26}$ powder prepared at 300 °C for the first three cycles. It can be seen that the CV curve of the first cycle is different from those of the subsequent cycles but the CV curve of the second cycle is similar to that of the third cycle. After the first cycle, the well defined cathode peaks located between 2.31 V and 2.93 V all disappear in the subsequent CV curves, which indicates that a structure modification may take place after the first cycle and should be responsible for the irreversible capacity above-mentioned. Therefore, it is believed that the structural modification of $Cu_{11}V_6O_{26}$ material caused by the irreversibility of Cu^{2+}/Cu couple is the origin of its capacity fading. Currently, the work of improving the cyleability of $Cu_{11}V_6O_{26}$ is under way, and will be reported elsewhere.

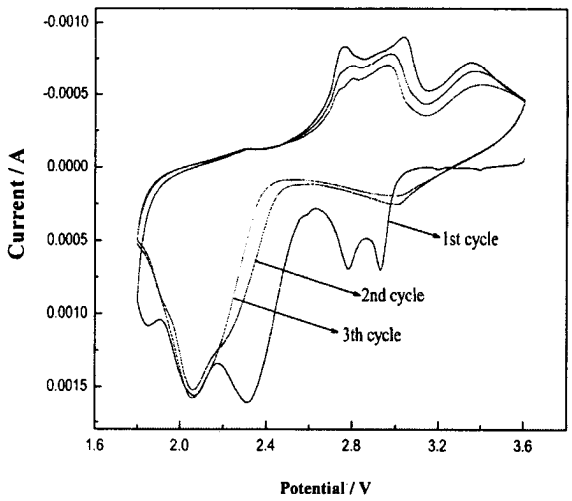

Fig. 6: Cyclic voltammograms of $Cu_{11}V_6O_{26}$ powder obtained at 300 °C.

Experimental

$Cu_{11}V_6O_{26}$ powders were synthesized by the oxalic acid–assisted liquid phase evaporation method. The whole processing included the following steps: firstly, $Cu(NO_3)_2$, NH_4VO_3 and $C_2H_2O_4{\cdot}2H_2O$ were dissolved in distilled water, in the molar ratio of 11:6:14. Oxalic acid was used as the chelating agent. Subsequently, the three solutions were mixed in a beaker. Secondly, the mixed solution was evaporated until the slurry residue was obtained. Then the slurry was allowed to dry at 120 °C followed by grinding, which gave rise to a powder, referred to as the $Cu_{11}V_6O_{26}$ precursor. Finally, an alumina crucible as container, the precursor was heated in tube-type

furnace at 300 °C ~ 500 °C for 10 h in an air atmosphere, and then cooled to room temperature. All the reagents were analytical reagent grade and as received.

X–ray diffraction (XRD) analysis was carried out on an XRD–Pert Pro diffractometer (XPERT PRO MPD, Netherlands) with Co Kα radiation (λ = 1.78901 Å) to identify the structure of the synthesized powders. The morphological feature of the as–prepared powders was observed on the SEM-JSM6380LA (JEOL, Japan). The analysis of particle size and particle size distribution was carried out with Mastersizer-2000 (Malvern instruments, England) using a laser granulometer based on a laser wavelength of 830 nm, power of 3 mW, and a multielement 42-channel detector. The discharge-charge performance of the thus-synthesized powders was assessed in CR2016 coin cells. The cathode film were composed of powders prepared above, acetylene black (AB) and polytetrafluoethylene (PTFE) binder at a weight ratio of 80:10:10. The working electrode was prepared by compressing the cathode film on stainless-steel collector. The CR2016 coin cells were assembled with pure lithium foil as a counter electrode, Celgard-2400 as the separator and 1 mol/L $LiClO_4$ dissolved in ethylene carbonate (EC) and dimethyl carbonate (DMC) solution (v/v, 1:1) as the electrolyte. Discharge-charge test of these cells at specific current of 30 mA/g between 1.8 V and 3.6 V was performed by a multi-channel Neware-battery tester (Neware, Shenzhen) at the ambient temperature. Cyclic voltammetry (CV) test was carried out on a CHI660A electrochemical workstation at a scan rate of 0.05mV/s using lithium foils as the reference and the counter electrodes.

Conclusion

$Cu_{11}V_6O_{26}$ cathode powders were prepared by the oxalic acid–assisted liquid phase evaporation method. The powder synthesized at 300 °C for 10 h shows the higher first discharge capacity (318.2 mAh/g) at 30 mA/g with a cut–off voltage of 1.8 V. Therefore, this novel synthesis method not only provides an alternative to synthesizing the high–capacity $Cu_{11}V_6O_{26}$ material *via* the low-temperature process but also is feasible in preparing other CVOs by varying the molar ratio of Cu:V. However, the capacity retention of the material is not as good as desired, which should be ascribed to the structural modification of $Cu_{11}V_6O_{26}$ material caused by the irreversibility of Cu^{2+}/Cu couple. Further work in improving the cycleability of $Cu_{11}V_6O_{26}$ cathode material needs to be done in order to make it achieve any practical application in lithium secondary batteries.

References

1. B. M. Winter, J. O. Besenhard, M. E. Spahr and P. Novák, *Advanced Materials*, **10**, 725 (1998).
2. Y. Sakurai, H. Ohtsuka and J. I. Yamaki, *Journal of the Electrochemical Society*, **135**, 32 (1988).
3. D. Ilic and D. Neumann, *Journal of Power Sources*, **43**, 656 (1993).
4. M. Eguchi, T. Yokoyama, T. Miura and T. Kishi, *Solid State Ionics*, **74**, 269 (1994).
5. E. Andrukaitis, J. P. Cooper and J. H. Smit, *Journal of Power Sources*, **54**, 465 (1995).
6. M. Eguchi, T. Iwamoto, T. Miura and T. Kishi, *Solid State Ionics*, **89**, 109 (1996).
7. M. Eguchi, A. Komamura, T. Miura and T. Kishi, *Electrochimica Acta*, **41**, 857 (1996).
8. E. Andrukaitis, *Journal of Power Sources*, **68**, 656 (1997).
9. F. Coustier, G. Jarero, S. Passerini and W. H. Smyrl, *Journal of Power Sources s*, **83**, 9 (1999).
10. M. Kamata, G. Oriji, Y. Katamaya, T. Miura and T. Kishi, *Solid State Ionics*, **146**, 95 (2002).
11. X. Y. Cao, J. G. Xie, H. Zhan and Y. H. Zhou, *Materials Chemistry and Physics*, **98**, 71 (2006).
12. X. Y. Cao, J. G. Xie, H. Zhan and Y. H. Zhou, *Journal of New Materials for Electrochemical Systems*, **9**, 47 (2006).
13. H. X. Li, L. F. Jiao, H. T. Yuan, M. Zhao, M. Zhang and Y. M. Wang, *Materials Letters*, **61**, 101 (2007).
14. H. Ma, S. Y. Zhang, W. Q. Ji, Z. L. Tao and J. Chen, *Journal of the American Chemical Society*, **130**, 5361 (2008).